Electronic Supplementary Information

Peptide-mediated Al(III) (oxy)(hydr)oxide formation: The specific stages of phase separation for additive interactions matter

Miodrag J. Lukić,[1,2]* Nele Marquardt,[1] Tim Schmalz,[1,3] Denis Gebauer[1]*

[1]Institute of Inorganic Chemistry, Leibniz University Hannover, Germany

[2]Laboratory of Physics, "Vinca" Institute of Nuclear Sciences, National Institute of the Republic of Serbia, University of Belgrade, Serbia

[1,3]Institute of Radioecology and Radiation Protection (IRS), Leibniz University Hannover, Germany

*Corresponding authors: Prof. Dr. Denis Gebauer: gebauer@acc.uni-hannover.de

Dr. Miodrag J. Lukić: miodrag.lukic@vin.bg.ac.rs

Table of contents

1. EXPERIMENTAL

1.1 Titration experiments

The early stages of Al(III) (oxy)(hydr)oxide formation were studied by employing pH-constant titration assays at low driving forces for phase separation using an OMNIS titration setup (Metrohm, Switzerland). The investigated pH range spanned from a mildly acidic to neutral region, i.e., from 3 to 7. The pH of the starting solution was adjusted using 0.05 M NaOH (Roth, Germany) and 0.1 M HCl (Roth, Germany) solutions. A 0.1 M solution of $AlCl_3 \cdot 6H_2O$ (Sigma Aldrich, Lot#STBJ0630) in 0.1 M HCl was dosed at a dosing rate of 0.01 ml/min in 35 ± 1 mL (App. I) or 0.02 ml/min in 70 ± 1 mL (App. II) of the starting solution. The influence of poly-L-aspartic acid (pAsp20) sodium salt (Mw = 2800 g/mol, Lot#109700207, Nanosoft polymers, USA) peptide on the nucleation of Al(III) (oxy)(hydr)oxide was studied. pAsp20 was used as received, without further purification. The experiments were performed in two experimental designs, Figure S1. The solids used for further analysis after App. I experiments in the final stage were derived after dosing 1.2 ml of the 0.1 M Al(III) solution, which equals 0.12 mmol or 3.24 mg of Al(III). The pAsp20 concentration present in the solution in App. I was 0.15 ± 0.005 mg/ml, which equals 5.25 ± 0.15 mg, while in the experiments addressing the concentration effect, this amount was varied from 0.35 mg (0.01 mg/ml) and 1.75 mg (0.05 mg/ml) to 17.5 mg (0.5 mg/ml); in App. II, the Al(III) system was driven to specific hydrolysis/phase separation points at pH 4.5; we have probed one experimental point before phase separation (BPS) and several experimental points after phase separation (APS). APS I was selected as the point immediately after phase separation to demonstrate the importance of controlling the Al(III) hydrolysis/phase separation for the interaction with the model peptide although the differences in the Al (III) concentration were little; other APS states were selected to show the magnitude of the effect, keeping the amounts of used Al(III) in the two experimental approaches comparable. The amount of added Al(III) in BPS, APS I, APSII, and APS III states was 0.9, 1.8, 3.24, and 6.48 mg, respectively, which corresponds to the experimental times of 1000, 2000, 3600, and 7200 s; thus, the APS II state was equivalent to the final App. I state with respect to the total amount of Al(III). It should be noted that the final Al(III) concentration in App. I is ~2.96 mM, while in App. II, it is ~0.45, 0.93, and 1.62 mM in BPS, APS I, and APS II states before adding pAsp20; in App. II, 20 ml of pAsp20 at a concentration of 0.5 mg/mL was added, which equals 10 mg of pAsp20 in total. The doubled dosing rate of the Al(III) solution in App. II experiments does not induce any significant kinetic effect as shown elsewhere,[1] and is effectively the same since the volume in App. II is twice of that in App. I, enabling the experimental scale-up to produce enough powder for characterization. At pH 5 in App. II, a volume of 1.2 ml of the 0.1 M Al(III) solution was added at a dosing rate of 0.01 ml/min, the volume was 35 ml, i.e., same as in App. I, and 10 ml of the pAsp20 was dosed, to demonstrate the experimental flexibility of the approach. For App. I, pAsp20 solutions were made by dissolving pAsp20 in MilliQ water, and the pH was adjusted with minor amounts of 0.1 M HCl and 0.05 M NaOH before each experiment. The acidic Al(III) solution was dosed into the pAsp20 solution (App. I) at the adjusted pH value, and the pH drop was automatically compensated by adding 0.05 M NaOH in the titration system. For App. II, the pH of pAsp20 solutions was pre-adjusted to the pH value of the experiment, so any change of pH upon dosing originated solely from Al(III) hydrolysis and the interaction with pAsp20 and not from the neutralization reaction. The pH electrode was calibrated on each experimental day using three buffers (pH 4.01, 7.00, and 9.21, Mettler, Toledo, Spain), and in between measurements, it was immersed in 0.1 M HCl for at least 30 min to remove any traces of Al(III) species eventually attached on the electrode's glass membrane. After titrations, samples were isolated by the following centrifugation sequence: 15 min at 9000 rpm to spin down the precipitate, then, the supernatant was decanted (or drawn for the ICP-OES analysis, please see below); afterwards, an HCl solution at the same pH value as the one in the actual experiment was added to remove Na^+ ions but not to induce any additional Al(III) hydrolysis/precipitation by changing the pH value, and then, centrifugation for 15 min at 9000 rpm was repeated; finally, the precipitate was washed with MiliQ water to remove any traces of remaining Cl^- ions by centrifuging again in the same manner; after decanting, the precipitate was left to dry overnight in an oven at 40 °C under air. Before analysis, the solid precipitate was pulverized in an agate mortar. It should be noted that samples derived in App. I were strongly sticking to the agate and pestle, while those from App. II were more rigid. The presented titration experiments were performed under temperature-controlled conditions at 25 °C, at least in triplicate and average curves are shown. For the effect of changing the pAsp20 concentration in App. I, keeping in mind that all experiments are performed in the same way with just different pAsp20 concentrations and that all fall ideally on the same curve after phase separation, Figure S4, some measurements were not repeated to reduce experimental time and cost. In pH evolution experiments, Figure S6,

after the pAsp20-free Al(III) system reached the APS II state, we stopped further Al(III) addition and compensated the pH drop up to 60 ks by counter-titrating with 0.05 M NaOH, and expressed it as c_{ex}(NaOH) vs. time. By keeping the same ionic strength as in experiments with Al(III) following App. I, we tested the behavior of NaCl, $CaCl_2$, and $FeCl_3$, Figure S10, demonstrating that Al(III) caused way stronger interaction than other metals, also Fe(III) (as determined from the volume of consumed NaOH), and that only Al(III) induced sudden pAsp20 precipitation.

1.2 Physical-chemical characterisation

FTIR spectra were acquired in ATR configuration (Vertex 70 FTIR, Bruker, Germany). A small amount of powder samples was placed onto the crystal surface, and pressed with a clamp, and the chamber was evacuated to avoid the influence of CO_2 from the air. The spectra were recorded in the transmittance mode, from 4000 to 400 cm^{-1}, with a resolution of 1 cm^{-1}, and 64 scans per spectrum. All spectra were baseline-corrected and normalized to 1, where the value of 0 corresponds to the baseline.

The morphology and particle size of the precipitated powders were characterized using a field-emission scanning electron microscope (Regulus 8230, HITACHI, Japan) equipped with an EDX detector for chemical analysis. The imaging was performed using secondary electrons at 5 kV and 10 μA. The samples were drawn from the titration vessel after the end of the experiment, filtrated using a 50-nm nitrocellulose filter paper, dried overnight and imaged on the paper with a carbon pad on the SEM holder stubs. The EDX acquisition time was 180 s, i.e., until the relative ratio of elements reached a ratio that practically did not change further. For determining the at.% of Al in the sample, the absolute amount of Al(III) or other relative ratios could not be used because it is scaled to the amount of C, where some part of the latter can also originate from the filter (also containing oxygen and a minor amount of N) used to isolate the sample or carbon conductive pad, the contributions of which should not be neglected. Thus, the Al/N ratio on clearly defined spots was used to assess the relative contribution of Al(III) and pAsp20 in the final solid.

Thermal analysis of Al(III)-pAsp20 solids derived after titration experiments was performed in an oxidative atmosphere (80 % N_2 – 20 % O_2) to 1000 °C, at a heating rate of 10 K/min (Jupiter, STA, Netzsch, Gemrany).

The amount of Al(III) involved in the interaction with pAsp20 was determined using inductively-coupled plasma optical emission spectroscopy, ICP-OES (PerkinElmer, US). The device was previously calibrated with a series of Al(III) nitrate solutions from 0 to 25 ppm made by dilution from a 100 ppm Al(III) ICP standard (Certipur®, 1.70301.0100, Merck) prepared using double-distilled 2.5 % HNO_3. The whole volume of the sample after titration experiments was quantitatively transferred into 50-ml cuvettes and centrifuged for 15 min at 9000 rpm to separate the precipitate from the supernatant solution. At such centrifugation rates/times, Al(III) species are not expected to spin down. 1 ml of the supernatant solution was taken and diluted 10 times by 2.5 % HNO_3 for ICP-OES measurements. The amount of Al(III) determined by ICP-OES was subtracted from the theoretically added amount, representing the amount of Al(III) involved in the interaction with pAsp20. The average values were taken from 3 measurements. All data are listed in Table S1.

1.3 Assessment of interaction energetics by isothermal titration calorimetry (ITC)

ITC (MicroCal-PEAQ-ITC, Malvern, UK) was used to assess the thermodynamics and binding parameters of Al(III) species to organic molecules. It directly measures the heat evolved or consumed during the interaction by comparing it to the heat supplied to a reference cell at constant temperature. It is performed by a controlled dosing of an injectant (here, Al(III) solution) into a cell that contains a sample (here, pAsp20 solution) under constant stirring and temperature. The method is highly sensitive to the smallest heat exchange and pH variations, so the use of buffers is recommended. In previous ITC studies on the interactions of the Al(III) system with organic molecules, different buffers were used to prevent pH changes: 0.1 M NH_4-acetate buffer in the pH range from 3.5 to 7 [2,3], or TRIS at pH 7 and MES at pH 4 [4]. Nevertheless, the “inertness” of the buffer has to be understood so that any interaction with the buffer is minimized. The rationale behind our experimental design is to complement the titration experiments and understand the dependency of the interactions on the distinct stages of Al(III) hydrolysis. As Al(III) species are highly reactive with molecules containing different functional groups, including

those of potential buffers, we have assessed the interaction of Al(III) with pAsp20 across a pH range from 3.0, 4.0, 4.5, to 5.0. At pH 7, solid $Al(OH)_3$ forms early, complicating the ITC measurements further, so this experimental point was not studied. The first set of experiments was done at pH 4.5 using 0.1 M NH_4-acetate buffer, as suggested in literature[2]. A 1 mM Al(III) solution was prepared by diluting an appropriate amount of a 10 mM Al(III) solution at pH 2 (0.01 M HCl, to avoid Al(III) hydrolysis) in the 0.1 M NH_4-acetate buffer at pH 4.5. The pAsp20 solutions were prepared from 0.5 mg/mL pAsp20 solutions at pH 4.5 by dissolving appropriate amounts in the 0.1 M NH_4-acetate buffer at pH 4.5, reaching the final pAsp20 concentration, optimized for ITC measurements, of $35.70 \cdot 10^{-3}$ mM. In the second experimental design without buffers, an injectant 0.5 mM Al(III) solution was also prepared from a 10 mM Al(III) stock solution of Al(III) at pH 2 by diluting appropriate amounts in HCl solutions at pH 3.0, 4.0, and 4.5. For the experiment at pH 5.0, the same procedure was applied, but here, a 10 mM Al(III) at pH 3 was used, and diluted in HCl at pH 5.0 to prepare a suitable injectant solution. Such approach brings the pH value of the dosing Al(III) solution close to the experimental pH value (with a difference < 0.5-1.0 pH unit), so that its dosing does not cause considerable pH changes that could affect the experimental data. It should be noted that both stock solutions when used at a concentration of 10 mM of Al(III) did not show any pH changes in between pH 2 and pH 3, demonstrating the absence of Al(III) hydrolysis. This experimental design enabled us to study the dosing of unhydrolysed or slightly hydrolysed Al(III) solutions to pAsp20 solutions, similar as in titration experiments, so the both reactions, Al(III) hydrolysis and Al(III)-peptide interactions are possible. Solutions prepared like this did not cause any critical pH change during ITC experiments and the data were fitted using a model available in MicroCal PEAQ-ITC analysis software, assuming heteroassociation and a one set of equivalent, non-interacting, binding sites available for Al(III) on the peptides, i.e., 1:1 stoichiometry, M+X = MX, where M stands for Al(III) and X for pAsp20. More data on the calculation of binding constant and binding parameters from the measured heat exchange can be found elsewhere.[5,6] Indeed, ITC experiments without buffer were way more sensitive than with buffer and the required Al(III) and pAsp20 concentrations were significantly smaller, enabling us to address the Al-peptide interaction without causing pAsp20 precipitation in the cell. An Al(III) concentration of 0.5 mM ensures that the system is still in the BPS stage up to pH 4.5, equivalent to titration experiments. The interaction energetics determined in the experimental design without buffers revealed considerably stronger thermodynamic effects, so the corresponding effects of the buffers should not be underestimated.

All ITC measurements were performed at 25 ± 0.1 °C. The cell volume was 280 µl, and the injectant (Al(III)) solution was dosed in 19 steps of 2 µl each, duration of 4 s, and the time space between injections was 150 s. To account for any side reactions like Al(III) hydrolysis and heats of dilution, we performed several control experiments: Al(III) dosing into HCl, dosing of HCl into HCl, and dosing of HCl into the pAsp20 solution. The first two control experiments were subtracted from the actual Al(III)-pAsp20 experiment, while the third was added to that data point-by-point. All thermodynamic parameters were determined from 3 separate experiments. The control titration experiments in the presence of the buffer at pH 4.5 revealed strong interactions, Fig. S10, plausibly due to the extra carboxylate groups of the buffer, advocating for the revisited experimental design.

2. Supplementary figures

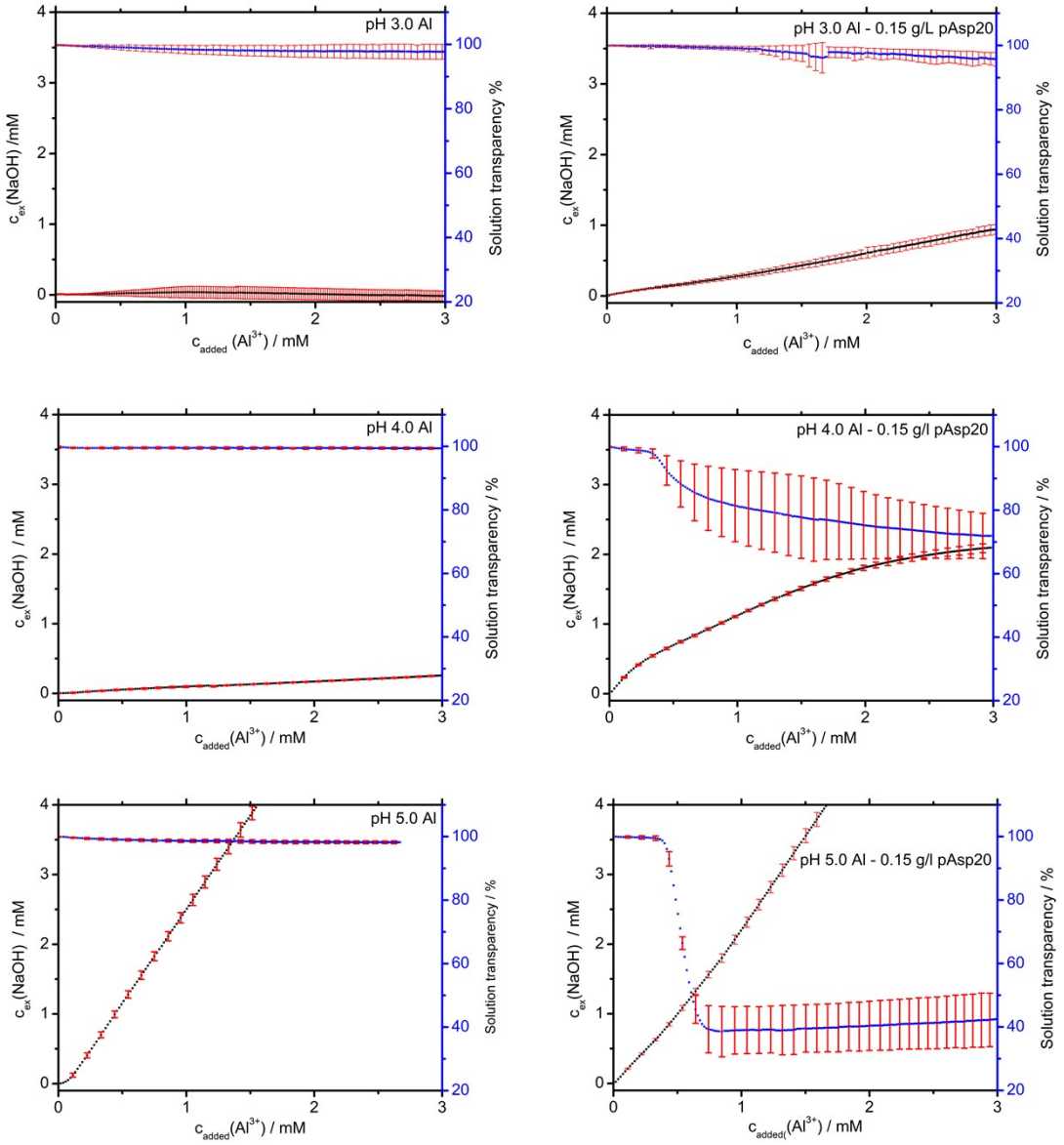

Fig. S1 Titration curves at pH 4.0 and 5.0 performed following App. I without and in the presence of 0.15 g/L pAsp20. The left y-axes of all graphs represent the concentration of excess added NaOH to keep the pH value constant, that is, originating only from Al(III) hydrolysis and/or interactions with pAsp20, as the amount of base added to compensate for the addition of the acidic Al(III) solution was subtracted in the corresponding calculations. The right y-axes (in blue), i.e., blue curves, of all graphs show the solution transparency determined by optoelectrode measurements at a wavelength of 610 nm, facilitating the determination of the onset of precipitation. Presented are the average curves from at least three experiments.

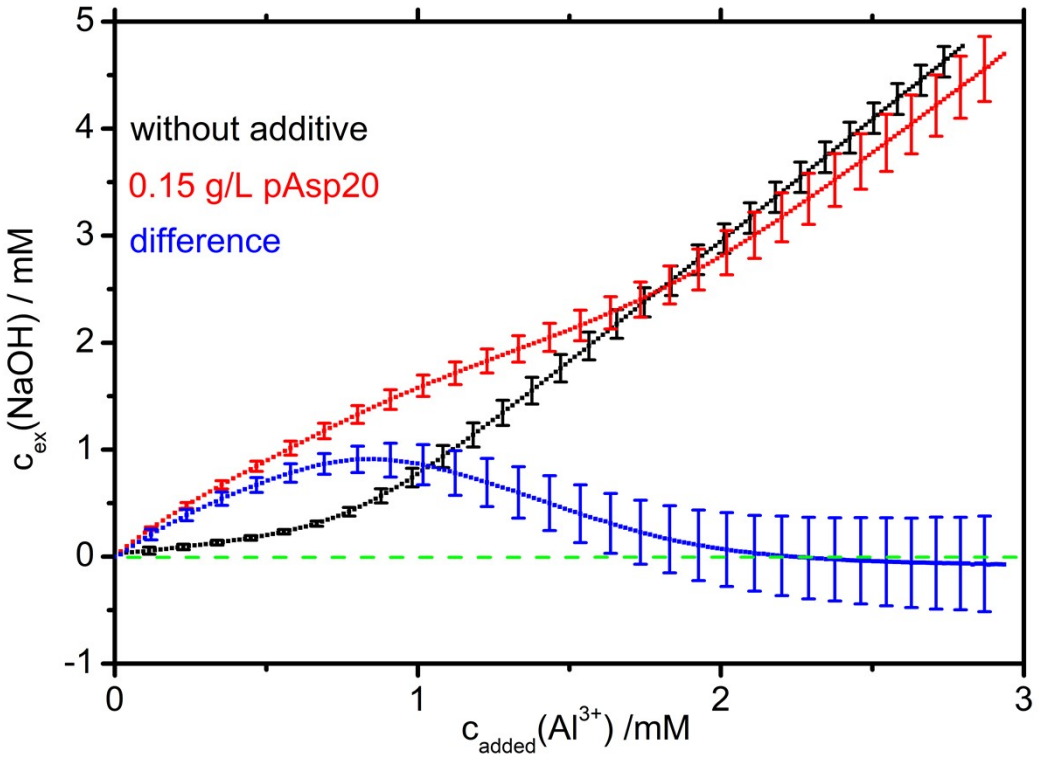

Fig. S2 Subtraction of the reference titration curve for the pure Al(III) system from the titration curve in the presence of 0.15 g/L of pAsp20 at pH 4.5 following App. I (Figure 1B), indicating slightly suppressed Al(III) hydrolysis upon the initial pAsp20 effect. A subtraction of averaged curves (N=3) was performed. The y-axis denotes the concentration of excess added NaOH to keep the pH value constant. The dashed green line is drawn through the zero point of the base consumption, i.e., it represents no difference in the base consumption compared to the reference system without pAsp20.

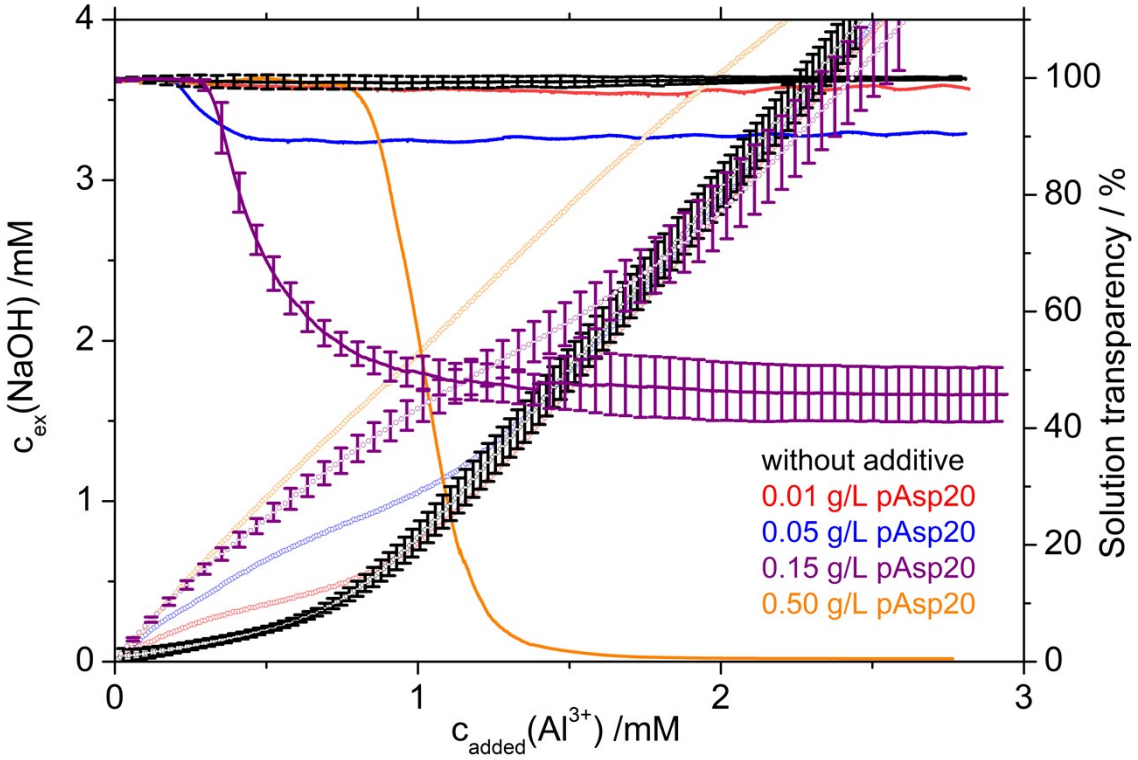

201

202 **Fig. S3** Concentration effect in App. I. Empty symbols represent titration curves, solid lines show solution
203 transparency curves.

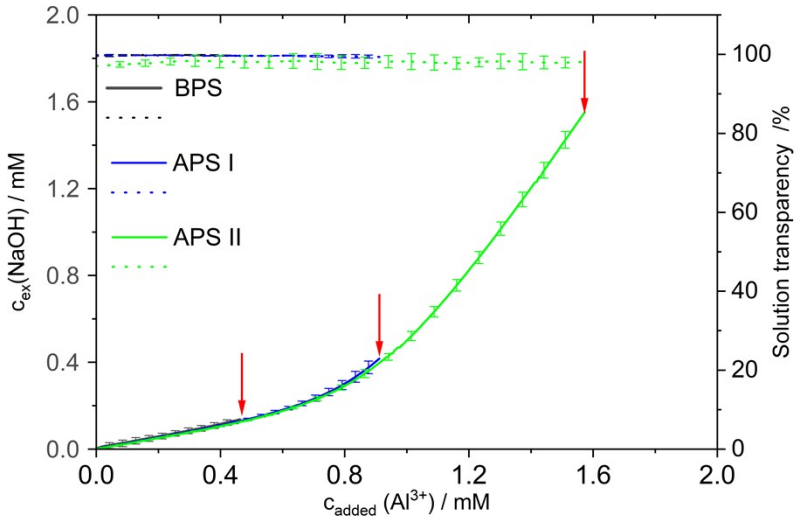

204

205 **Fig. S4** Titration curves of the pure Al(III) system at pH 4.5 titrated to the distinct hydrolysis/phase separation
206 states referred to as before phase separation (BPS) and after phase separation (APS) I and II. The Al(III) solutions
207 were carefully driven to the respective points (labeled by red arrows), representing the end-points of the titration
208 curves, which were afterwards immediately titrated with pAsp20 solutions with a concentration of 0.5 mg/mL at
209 the same pH value. The NaOH titration was continued so as to maintain this pH level upon the addition of the
210 pAsp20 solutions. Almost flat dotted curves in the upper part represent solution transparency signals (right y-axis)
211 measured by an optrode at 610 nm, showing basically no changes, since no visible precipitate forms in the solution,
212 i.e., the solution remains completely transparent.

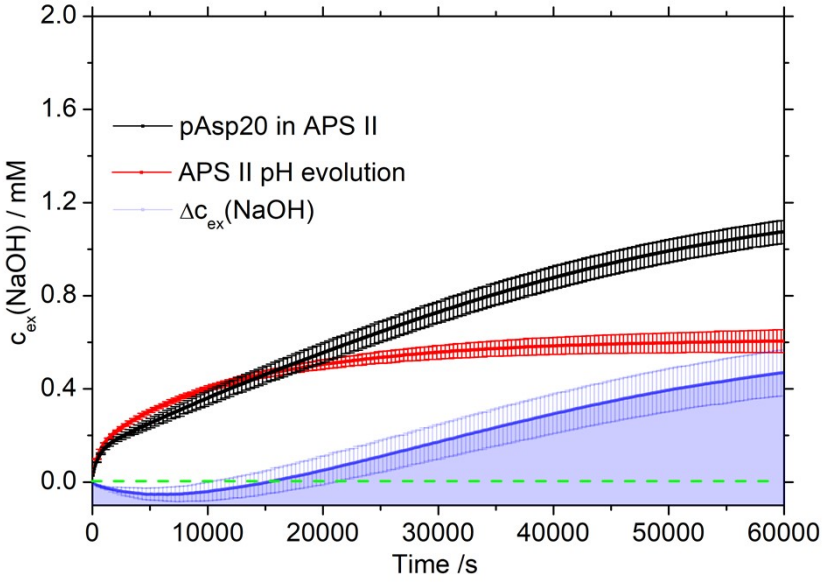

213

214 **Fig. S5** pH evolution experiments at pH 4.5. The pH evolution titration curve from the APS II states without
215 pAsp20 (*red curve*) and the titration curve with pAsp20 (*black curve*), and the final Δc(OH) curve (*blue curve*)
216 obtained after subtraction of the red from the black curve. All curves represent the average curves from at least
217 three experiments.

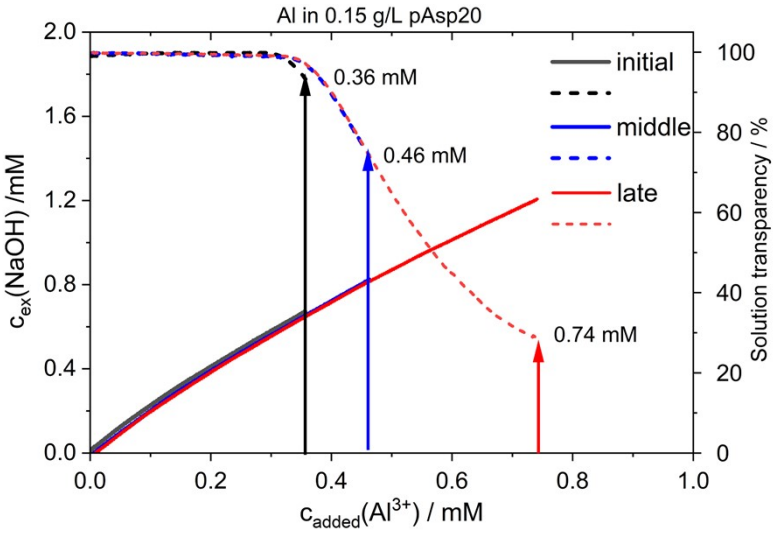

218

219 **Fig. S6** Sampling points indicated with arrows on titration curves according to App. I. Samples were drawn from
220 the titration experiments based on the transparency signal change (the right axis) of the solution in the initial
221 (*black*), middle (*blue*), and late (*red*) stages to investigate the chemical characteristics of the solids derived in the
222 early stage interaction between Al (III) species and pAsp20 (left panel) and pGlu20 (right panel) at pH 4.5. Al(III)
223 concentrations at the sampling points are indicated with respective numbers in the graphs. Solid lines represent
224 titration curves, dashed lines represent solution transparency curves.

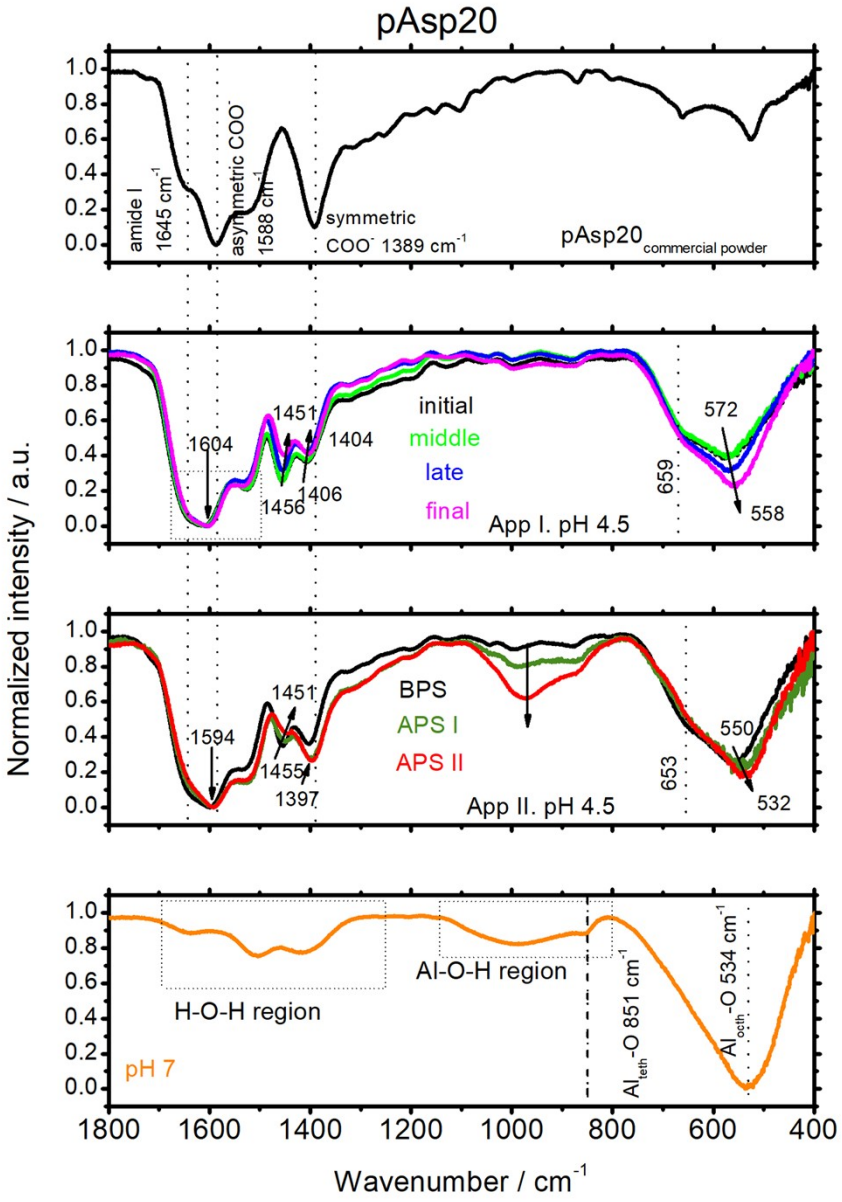

225

226 **Fig. S7** FTIR spectra of solids derived from titration experiments at pH 4.5 compared with commercial pAsp20
227 and amorphous $Al(OH)_3$ prepared at pH 7. (A) (*top*) pAsp20 commercial powder; (*second from top*) solids derived
228 from the initial (black), middle (green), and late (blue) stages (according to the transparency drop in the solution
229 (**Fig. S6**) during the titration of 0.15 g/L pAsp20 with acidic Al(III) solution, and the solid derived at the end of
230 the equivalent titration experiment (magenta) in App. I; (*second from bottom*) solids derived from the titration
231 experiments by dosing pAsp20 in the BPS (black), APS I (olive) and APS II (red) stages following App. II;
232 (*bottom*) the reference amorphous $Al(OH)_3$ prepared at pH 7.

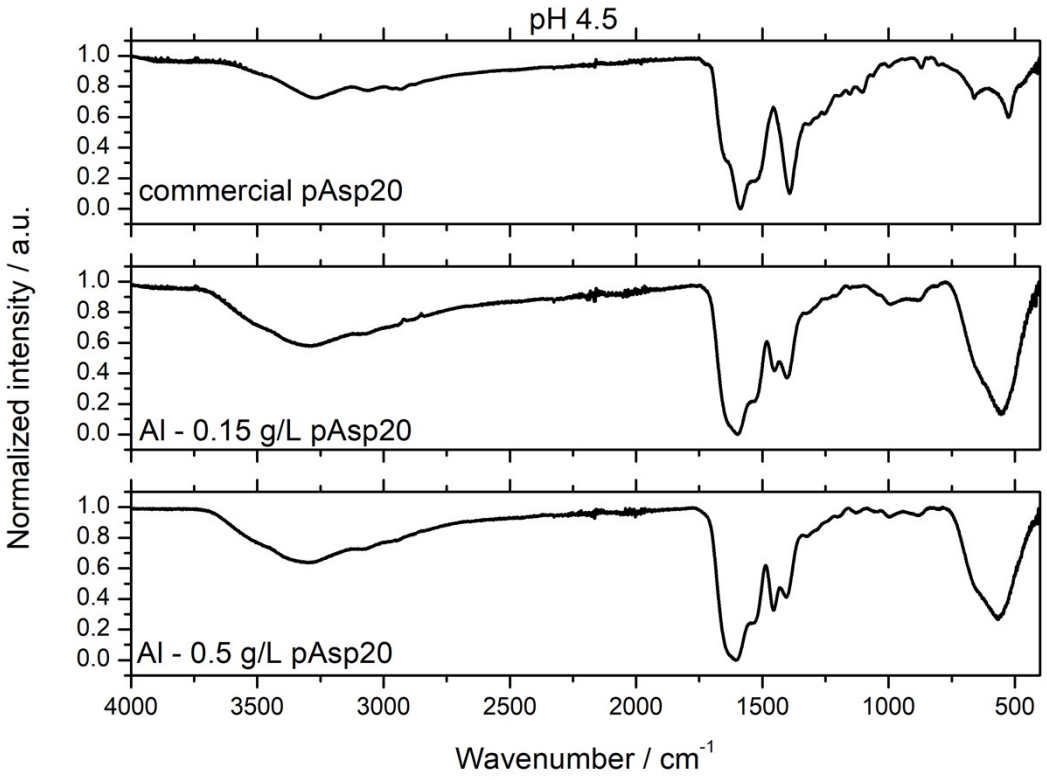

Fig. S8 FTIR spectra of the solids derived at pH 4.5 with different pAsp20 concentrations in App. I.

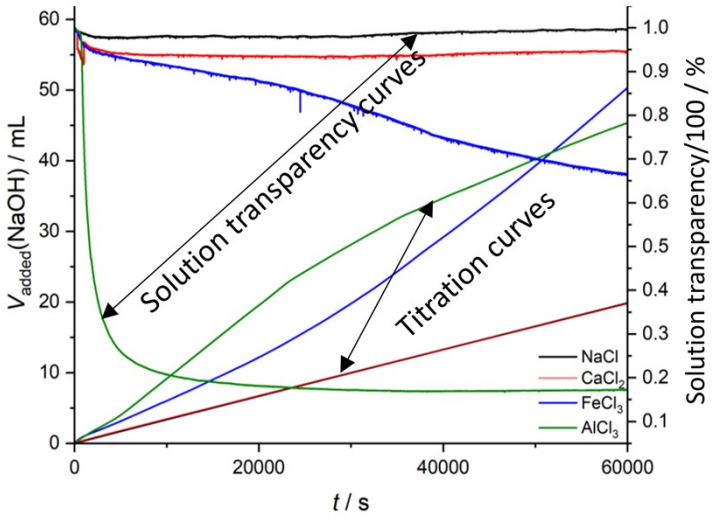

Fig. S9 Volume of consumed NaOH (to keep the pH value constant during titration experiments) vs. time following App. I at pH 4.5 using NaCl, $CaCl_2$, and Fe(III)Cl_3 solutions of the same ionic strength as for $AlCl_3$. Al(III) induces sudden pAsp20 precipitation, unlike Fe(III), Ca(II) and Na(I).

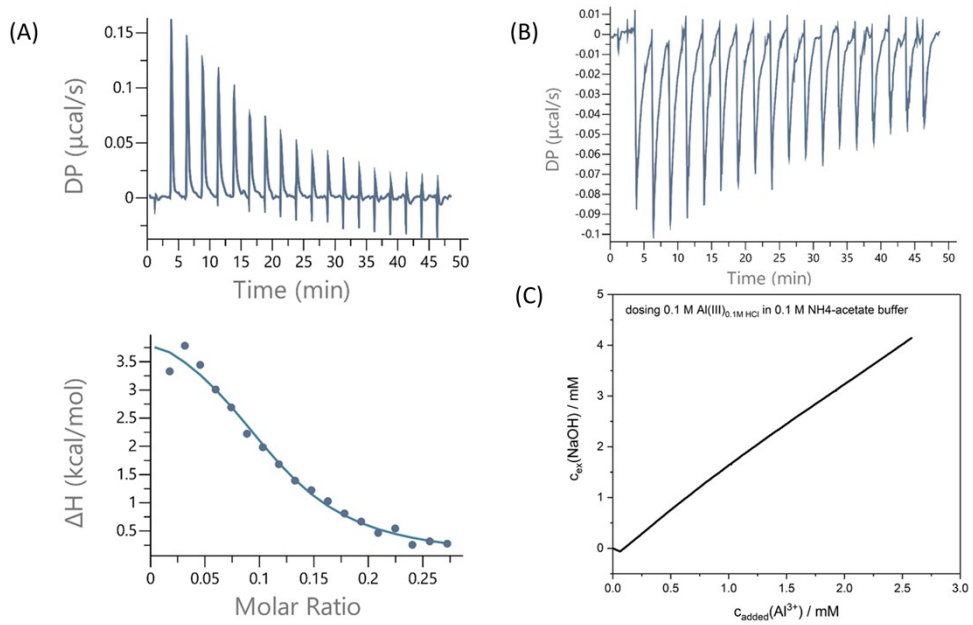

Fig. S10 The interaction of Al(III) with pAsp20 in the presence of 0.1 M NH_4-acetate buffer: ITC traces of dosing (A) buffered Al(III) in buffered pAsp20 (0.1 M NH_4-acetate buffer), and (B) buffered Al (III) in the 0.1 M NH_4-acetate buffer as a control experiment, both at pH 4.5; (C) the titration experiment same as those used in App. I, dosing non-buffered Al(III) in the NH_4-acetate buffer, indicating strong interaction, i.e., strong base consumption to keep the pH constant.

3. Supplementary tables

Table S1. ICP-OES analyses of the Al(III)-pAsp20 system at different pH values.

pH	$c_{remaining}(Al^{3+})_{ICP}$ / ppm	$m_{remaining}(Al^{3+})$ / mg	$m_{used}(Al^{3+})$ / mg	$m_{used}(Al^{3+})$ / %
4.0 App. I	59.1±6.0	2.38	0.86	26.5
4.5 App. I	58.37±0.13	2.45	0.79	24.3
5.0 App. I	55.13±1.20	2.46	0.78	24.1
4.5_App. II_APS II	13.94±0.38	1.36	1.88	58.0

$n_{added}(Al^{3+})$ = 0.12 mmol; $m_{added}(Al^{3+})$ = 3.24 mg;

4. References

[1] Lukić M J, Wiedenbeck E, Reiner H and Gebauer D 2020 Chemical trigger toward phase separation in the aqueous Al(III) system revealed *Science Advances* **6** eaba6878

[2] Wu J, Du F, Zhang P, Khan I A, Chen J and Liang Y 2005 Thermodynamics of the interaction of aluminum ions with DNA: Implications for the biological function of aluminum *Journal of Inorganic Biochemistry* **99** 1145–54

[3] Liang Y 2006 Applications of isothermal titration calorimetry in protein folding and molecular recognition *JICS* **3** 209–19

[4] Belliardo C, Di Giorgio C, Chaspoul F, Gallice P and Bergé-Lefranc D 2018 Direct DNA interaction and genotoxic impact of three metals: Cadmium, nickel and aluminum *The Journal of Chemical Thermodynamics* **125** 271–7

[5] Wiseman T, Williston S, Brandts J F and Lin L-N 1989 Rapid measurement of binding constants and heats of binding using a new titration calorimeter *Analytical Biochemistry* **179** 131–7

[6] Gindele M B, Malaszuk K K, Peter C and Gebauer D 2022 On the Binding Mechanisms of Calcium Ions to Polycarboxylates: Effects of Molecular Weight, Side Chain, and Backbone Chemistry *Langmuir* **38** 14409–21